Trio-based exome sequencing arrests de novo mutations in early-onset high myopia

Zi-Bing Jin[a,1,2], Jinyu Wu[b,1], Xiu-Feng Huang[a], Chun-Yun Feng[a], Xue-Bi Cai[a], Jian-Yang Mao[a], Lue Xiang[a], Kun-Chao Wu[a], Xueshan Xiao[c], Bethany A. Kloss[d], Zhongshan Li[b], Zhenwei Liu[b], Shenghai Huang[a], Meixiao Shen[a], Fei-Fei Cheng[a], Xue-Wen Cheng[a], Zhi-Li Zheng[a], Xuejiao Chen[a], Wenjuan Zhuang[e], Qingjiong Zhang[c], Terri L. Young[d], Ting Xie[f], Fan Lu[a,2], and Jia Qu[a,2]

[a]The Eye Hospital of Wenzhou Medical University, The State Key Laboratory of Ophthalmology, Optometry and Vision Science, Wenzhou 325027, China; [b]Institute of Genomic Medicine, Wenzhou Medical University, Wenzhou 325027, China; [c]State Key Laboratory of Ophthalmology, Zhongshan Ophthalmic Center, Sun Yat-sen University, Guangzhou 510060, China; [d]Department of Ophthalmology and Visual Sciences, University of Wisconsin–Madison, Madison, WI 53705; [e]Ningxia Eye Hospital, People's Hospital of Ningxia Hui Autonomous Region, Yinchuan 750021, China; and [f]Stowers Institute for Medical Research, Kansas City, MO 64110

Edited by Jeremy Nathans, Johns Hopkins University, Baltimore, MD, and approved February 27, 2017 (received for review September 29, 2016)

The etiology of the highly myopic condition has been unclear for decades. We investigated the genetic contributions to early-onset high myopia (EOHM), which is defined as having a refraction of less than or equal to −6 diopters before the age of 6, when children are less likely to be exposed to high educational pressures. Trios (two nonmyopic parents and one child) were examined to uncover pathogenic mutations using whole-exome sequencing. We identified parent-transmitted biallelic mutations or de novo mutations in as-yet-unknown or reported genes in 16 probands. Interestingly, an increased rate of de novo mutations was identified in the EOHM patients. Among the newly identified candidate genes, a *BSG* mutation was identified in one EOHM proband. Expanded screening of 1,040 patients found an additional four mutations in the same gene. Then, we generated *Bsg* mutant mice to further elucidate the functional impact of this gene and observed typical myopic phenotypes, including an elongated axial length. Using a trio-based exonic screening study in EOHM, we deciphered a prominent role for de novo mutations in EOHM patients without myopic parents. The discovery of a disease gene, *BSG*, provides insights into myopic development and its etiology, which expands our current understanding of high myopia and might be useful for future treatment and prevention.

early-onset high myopia | de novo mutations | *BSG* | rare inherited mutations

Myopia is the most common ocular disease, with an increasing global prevalence, especially in East Asia (1–3). Uncorrected myopia is the leading cause of vision impairment worldwide, according to a report by the World Health Organization (4). High myopia (HM) is very severe myopia, which is defined as less than or equal to −6.00 diopters (D) (5). HM is clinically associated with severe ocular complications, such as macular degeneration, retinal detachment, cataract, and glaucoma, which make HM the leading cause of irreversible blindness in East Asia (1, 6).

Myopia is etiologically heterogeneous because both environmental factors and genetic factors are involved (1, 7). Epidemiological surveys show that outdoor activity reduces the prevalence of myopia, decreasing the risk of myopia associated with short-distance work (8, 9). Myopia often exhibits apparent familial aggregation (10–12), and the number of myopic parents is significantly correlated with myopic onset and progression in children (13). Twin studies and population-based epidemiological investigations show that genetic factors significantly contribute to the development of myopia (6, 14, 15), particularly HM (5). Genome-wide association studies (GWAS) and subsequent metaanalyses have identified dozens of loci and genes that are associated with general myopia or HM (16, 17). Of note, the identified genetic contributions of the dozens of loci and genes to myopia are very limited. To date, based on pedigree studies with next-generation sequencing, several disease-causing genes have been discovered, including two recessive genes, *LRPAP1* (18) and *LEPREL1* (19); four dominant genes, *ZNF644* (20), *SCO2* (21), *SLC39A5* (22), and *P4HA2* (23); and one X-linked gene, *ARR3* (24). However, a large-scale screening of these genes in HM cohorts provided evidence that only a small proportion (<5%) of HM patients harbor mutations in these known genes, which can be attributed to as-yet-unidentified causative genes (25).

Because preschool children encounter fewer risks from environmental pressures, we proposed that the condition of early-onset high myopia (EOHM) is driven by a genetic predisposition more than by environmental factors. In this study, we recruited 18 familial trios (healthy parents and an EOHM child) to decipher the genetic predisposition using whole-exome sequencing (WES). We identified a cluster of unique genes linked to EOHM, as well as mutations in the reported genes. Notably, we showed that both rare inherited mutations and de novo mutations significantly contributed to EOHM. Expression profiling in ocular tissues and mutant mouse phenotyping demonstrated the

Significance

Because preschool children encounter fewer risks from environmental pressures, we propose that the condition of early-onset high myopia (EOHM) is driven by a genetic predisposition more than by environmental factors. In this study, we recruited 18 familial trios to decipher the genetic predisposition using whole-exome sequencing. We identified a cluster of unique genes linked to EOHM, as well as mutations in the reported genes. Notably, we showed that both rare inherited mutations and de novo mutations significantly contributed to EOHM. Expression profiling in ocular tissues and mutant mouse phenotyping demonstrated the pathogenicity of mutations in a unique gene, *BSG*. Our results provide insights into the genetic basis and molecular mechanisms of childhood high myopia.

Author contributions: Z.-B.J., J.W., F.L., and J.Q. designed research; Z.-B.J., J.W., X.-F.H., C.-Y.F., X.-B.C., J.-Y.M., L.X., K.-C.W., F.-F.C., X.-W.C., X.C., and T.X. performed research; Z.-B.J., J.W., X.X., B.A.K., M.S., W.Z., Q.Z., T.X., F.L., and J.Q. contributed new reagents/analytic tools; Z.-B.J., J.W., X.-F.H., Z. Li, Z. Liu, S.H., Z.-L.Z., and T.L.Y. analyzed data; and Z.-B.J., J.W., and X.-F.H. wrote the paper.

The authors declare no conflict of interest.

This article is a PNAS Direct Submission.

Freely available online through the PNAS open access option.

Data deposition: The sequencing data have been deposited in the figshare database, https://figshare.com/s/0eab58f90f3b1b20a181 (DOI: 10.6084/m9.figshare.3497660).

[1]Z.-B.J. and J.W. contributed equally to this work.

[2]To whom correspondence may be addressed. Email: jinzb@mail.eye.ac.cn, jqu@mail.eye.ac.cn, or lufan@mail.eye.ac.cn.

This article contains supporting information online at www.pnas.org/lookup/suppl/doi:10.1073/pnas.1615970114/-/DCSupplemental.

pathogenicity of the mutations in a unique gene, *BSG*. Our results provide insights into the genetic basis and molecular mechanisms of childhood HM.

Results

EOHM Samples and WES. In this study, we recruited a cohort of 54 individuals, including 18 children with EOHM and their unaffected parents. The ages at examination of all probands were less than 6, indicating EOHM. The refraction of each patient was less than or equal to −6.00 diopters (D) (Table S1).

WES was performed for all probands and the parents of the 18 trios to investigate the genetic basis. Burrows–Wheeler transform (26) and Genome Analysis Toolkit (GATK) (27) were used for the data analyses. The detailed statistical information of the WES data from the 18 HM trios is summarized in the Table S2.

Rare Inherited Mutations in EOHM. Rare inherited mutations cause HM in an autosomal recessive, dominant, or X-linked manner. Based on the sporadic EOHM patients used in this study, we first tried to identify biallelic mutations using mirTrios (28). We identified two known HM candidate genes (*LEPREL1* and *GRM6*), three oculopathy-related genes (*FAM161A*, *GLA*, and *CACNA1F*), and a further possible gene (*MAOA*) in six different individuals, which accounted for one-third of the EOHM samples (Dataset S1 and Table S3).

In proband H16, we detected a damaging biallelic mutation (p.L530P) in *LEPREL1*, which is involved in collagen chain assembly, stability, and cross-linking. Mutations in this gene have been reported in patients with HM in western Asia (19, 29) and China (30). *Leprel1* knockout (KO) mice with abnormal collagen chemistry partially recapitulate the myopic changes (31). Proband H33 carries a homozygous mutation (p.Q708H) in the *GRM6* gene. Mutations in *GRM6* are reported in HM (32) and nyctalopia (33). In addition to these two known genes, we identified a unique candidate gene, *FAM161A*, which is involved in microtubule stabilization (34, 35). Proband H45 harbors a nonsense mutation (p.Q302X) in *FAM161A*. Loss-of-function mutations in this gene are reported to cause autosomal recessive retinitis pigmentosa (36, 37). Interestingly, HM is coupled with these diseases in patients (38).

In another three unrelated patients, we detected mutations in three candidate genes, including *MAOA*, *GLA*, and *CACNA1F*. A boy (H1) harbored a hemizygous mutation in *MAOA* (p.V18E), which encodes an oxidative deaminase for amines. It is reported that 5-hydroxytryptamine is involved in the development of retinal ganglion cells (39, 40). In addition, we identified a hemizygous mutation (p.Y216F) in the galactosidase α (*GLA*) gene in proband H9. This gene is a known candidate gene for Fabry disease with an ocular pathology (41) and corneal dystrophy (42). Furthermore, a hemizygous mutation in the *CACNA1F* gene (p.R1060W) was discovered in proband H29. *CACNA1F* mutations are reported in patients with HM, congenital stationary night blindness type 2A (43), cone–rod dystrophy (44), and nyctalopia (45).

Contribution of the de Novo Mutation to EOHM. With the exception of the rare inherited mutations described above, we propose that de novo germline mutations may contribute to the genetic architecture of EOHM, which has not been fully studied. Using the Burrows–Wheeler Aligner (BWA)/GATK/mirTrios, we identified a total of 29 de novo single-nucleotide variants (SNVs) within the coding regions. We confirmed that 20 of the 29 de novo SNVs were genuine de novo mutations by direct PCR sequencing, and 17 were identified as nonsynonymous mutations (Dataset S2). Overall, 13 of the 18 probands (72%) carried at least one de novo mutation, and 7 probands harbored (39%) more than two de novo mutations.

The overall de novo mutation rate in the probands (1.11 events per proband on average) was consistent with a background de novo mutation rate of ∼0.91–1.07 that was estimated from previous studies (46–48). To determine whether the EOHM probands had elevated de novo mutations compared with the controls, we obtained the de novo mutation rates in the normal individuals from the NPdenovo database (49). As a result, we found an increased trend of the overall de novo mutation rate in the HM patients (1.11 events per proband on average) compared with that in the normal individuals (0.74 events per individual on average) with an HM/control rate ratio (RR) of 1.51 ($P = 0.05$) (Fig. 1*A*). Interestingly, we observed a significantly elevated de novo missense mutation rate in the patients compared with that in the normal individuals (RR = 1.98, 0.94 vs. 0.48, $P = 0.008$), and this difference was even greater (RR = 3.74, 0.39 vs. 0.1, $P = 0.004$) when only the damaging de novo missense mutations were considered. In addition, the number of de novo SNVs in each proband was significantly correlated with the paternal age ($r = 0.491$, $P = 0.019$) (Fig. 1*B*) using a Pearson correlation analysis, which is consistent with previous findings (50, 51). We correlated the number of de novo mutations detected and the degree of myopic refraction in each eye to analyze the possible direct contributions of the de novo mutations to the HM phenotypes. We observed a trend of a higher degree of myopia as the number of de novo mutations increased (0, one, and two) (Fig. 1 *C* and *D*).

Candidate Genes with Damaging de Novo Mutations. The detection of recurrent de novo mutations is a commonly used method to identify disease-causing genes. However, in this study, we found that the de novo mutations occurred in different genes in all cases, which prevented us from performing a statistical analysis of any of the specific genes. Therefore, we used 14 bioinformatics tools to predict the damaging effects of all missense de novo mutations detected and identified mutations that were more likely to confer a disease risk (Fig. 1*E*). One de novo missense mutation in the *EPHB2* gene was identified in proband H42, and the mutation was predicted to be damaging by 10 bioinformatics tools. The *EPHB2* gene is involved in retinal axon projections via interactions with ephrin-B proteins (52). In addition, it was reported that the growth cone collapse and axon retraction of retinal ganglion cells could be induced by *EPHB2* gene expression (53). Therefore, the direct evidence of the contribution of the *EPHB2* gene to retinal axon projections suggests that the *EPHB2* mutations may be a possible cause of the optical problems observed in the proband. One de novo missense mutation in the *CSMD1* gene was identified in proband H70, which is related to several neuron function-related disorders, such as schizophrenia, autism, sclerosis, etc. (54). One de novo missense mutation in the *TENM4* gene was identified in proband H1. Notably, the *TENM4* gene is also associated with neuron function-related disorders based on the genome sequencing of cases and controls (55) and a GWAS study (56). In addition, the *TENM4* gene is essential for embryonic mesoderm development in mouse model studies (57). One de novo missense mutation in the BSG gene was identified in proband H13. The BSG gene encodes a photoreceptor-specific transmembrane protein, Basigin, which cross talks with rod-derived cone viability factor (*RdCVF*) (58, 59). The BSG gene will be discussed further in the subsequent sections as a unique candidate gene for EOHM.

Expanded Screening Identified *BSG* Mutations. A mutation in the *BSG* gene (c.889G>A, p.G297S) identified in the EOHM patient (Fig. 2) showed strong pathogenicity, according to computational predictions. Moreover, it is completely absent in Exome Variant Server (EVS) and 1000 Genomes Project (1000G) and exhibits a very rare frequency in Exome Aggregation Consortium (ExAC) (1/115742, 8.64e-06). We further screened the entire coding region of the *BSG* gene in a large cohort of 1,040 unrelated patients with HM, none of which had mutations in the known genes, to determine the replication of the *BSG* mutations. Interestingly, we also identified one different missense

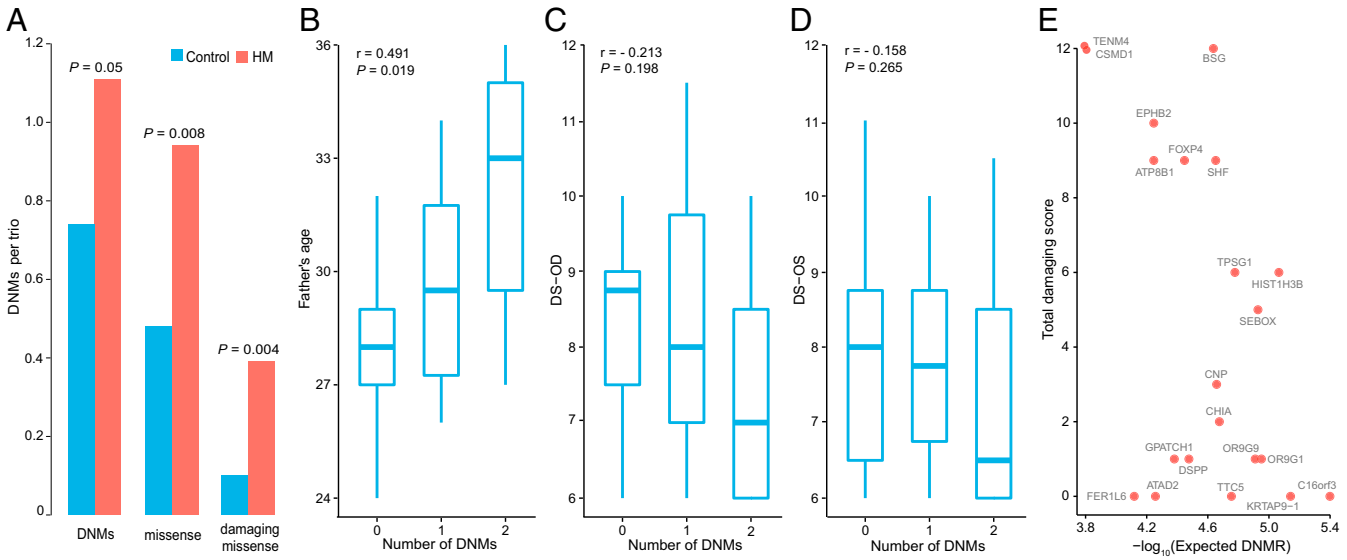

Fig. 1. Patterns of de novo mutations in HM patients and their contribution to disease risk. (*A*) Plot of the mean de novo mutation rate of HM patients (HM) and normal individuals (control). The de novo mutation rate for normal individuals was calculated based on 982 normal individuals from the NPdenovo database (www.wzgenomics.cn/NPdenovo/). The statistical significance of the differences in the de novo mutation rates between the HM patients and the controls was tested using a two-sample Poisson rate test. (*B*) The relationship between the number of de novo mutations and the paternal age. (*C*) The relationship between the number of de novo mutations in the proband and the diopter sphere–oculus dexter (DS-OD). (*D*) The relationship between the number of de novo mutations in the proband and the diopter sphere–oculus sinister (DS-OS). (*E*) A scatter diagram of the total damaging scores and the expected de novo mutation rate (expected DNMR) of the genes with de novo mutations. The total damaging score was calculated by 14 generic functional prediction tools, and the expected DNMR was used for each gene DNMR average from the mirDNMR database (www.wzgenomics.cn/mirdnmr/).

mutation (c.661C>T, p.P221S), one nonsense mutation (c.205C>T, p.Q69X), and one splicing mutation (c.415+1G>A) in the *BSG* gene (Table 1 and Fig. 2) in a total of four unrelated families. All of these mutations were absent in the ExAC database and either led to a protein coding change (c.205C>T, p.Q69X; c.415+1G>A) or displayed strong pathogenicity according to the computational assessment (c.889G>A, p.G297S; c.661C>T, p.P221S). Furthermore, both of the missense mutation (G297S and P221S) sites are located in highly conserved amino acids across different species (Fig. 2). However, because the parental DNA was unavailable, it is not clear

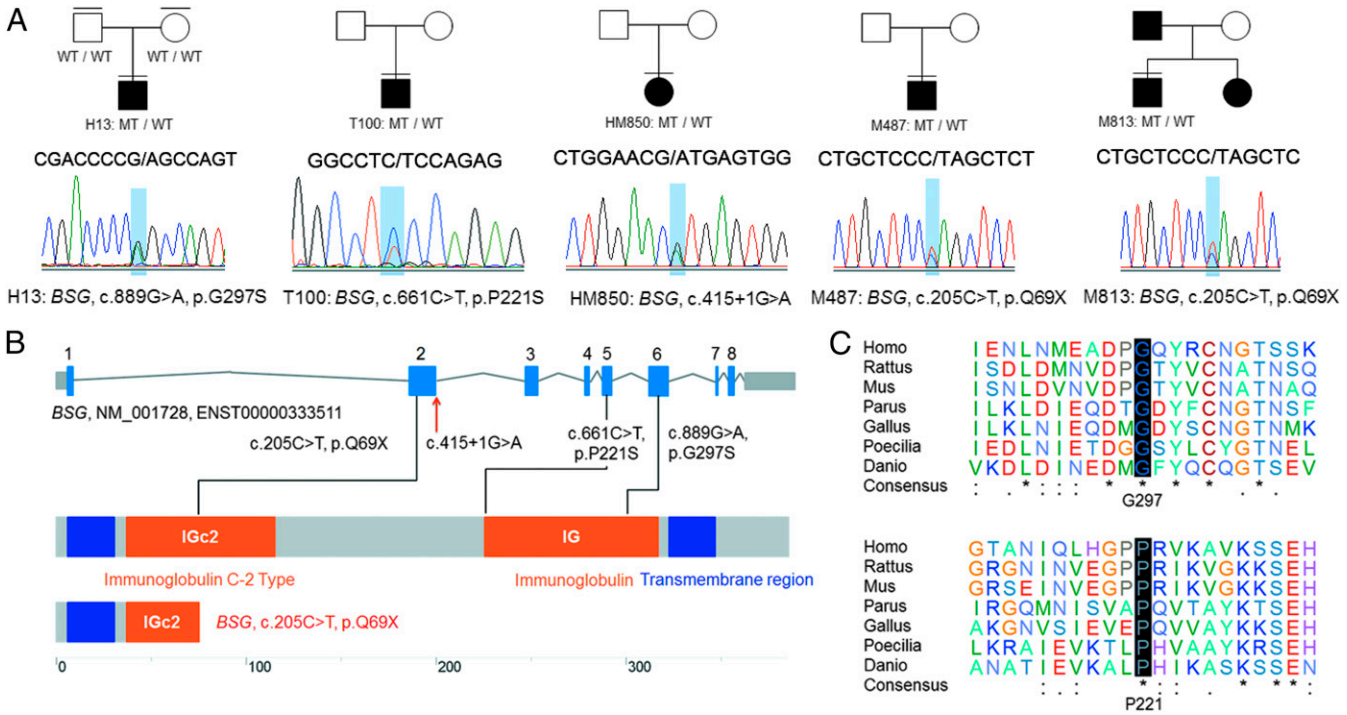

Fig. 2. Identification of mutations in the *BSG* gene. (*A*) Identification of mutations in the *BSG* gene in five unrelated patients. (*B*) Schematic of the *BSG* gene and its domains with the sites of the variants identified in this study. (*C*) Both missense mutations (G297S and P221S) are located in highly conserved regions.

whether these mutations are de novo mutations. Taken together, these results confirmed the recurrence of the *BSG* mutations by expanded screening in an additional HM cohort, which supported the pathogenicity of this gene for HM.

Bsg Mutant Mice Display Typical Myopic Phenotypes in the Axial Length. We generated knockin mice (Fig. S1) with a c.901G>A mutation corresponding to the c.889G>A mutation identified in the EOHM patient to further investigate the functional impact of the *BSG* mutation. The total axial length (AL) and vitreous chamber depth (VCD) were measured in variant ages (4, 6, 8, and 10 wk) of the mutant mice and wild-type (WT) siblings. The results showed that the ΔAL significantly changed with group (F = 51.26, P = 1.63e-10) and time (F = 42.36, P = 6.50e-14) overall, and there were no interactions between group and time (F = 2.35, P = 0.1012) (Fig. 3). The heterozygous mutant group had an increased AL in the subsequent 2 wk compared with the WT group (Tukey multiple comparison, Δmean = 0.015 mm, P < 1e-50). The ΔAL in the subsequent 2 wk also changed with time (peaks at 6 wk, and then the ΔAL decreased slightly). However, there were no significant differences with group (F = 0.47, P = 0.49) and time (F = 1.86, P = 0.16) in ΔVCD (Fig. S2). The trend of the AL and VCD of the WT mice was consistent with the previous studies as follows: AL increases during postnatal development, whereas the VCD decreases (60, 61).

To test whether retinal function was affected in the mutant mice, we performed an electroretinogram (ERG). The results showed that both the photopic and scotopic ERG responses of the mutant mice were normal compared with those of their WT siblings (Fig. S3). This result indicated that the retinal function was not affected by the *Bsg* mutation, which was consistent with the clinical manifestation in the patients. Taken together, the results showed that the *Bsg* mutant mice displayed typical HM phenotypes with a longer AL but no retinal dysfunction.

Spatial Expression Patterns of the *Bsg* Gene in Mice. Next, we wanted to determine the *Bsg* expression patterns in different tissues. Therefore, we investigated the spatial expression patterns of *Bsg* in various mouse tissues. Interestingly, two known myopia-related genes, *Sco2* and *Sntb1*, exhibited patterns similar to that of *Bsg* (Fig. S4).

Discussion

Both myopia and HM are etiologically heterogeneous disorders. It is commonly known that both genetic factors and environmental factors contribute to the etiology (1). Population-based epidemiological investigations found that the disease is associated with environmental risk factors, such as a close reading distance and less outdoor activity (8, 9). With the advent of next-generation sequencing, a few of disease genes have been discovered in recent years (18–24). Because myopia is dependent on both genetics and lifestyle and preschool children have less exposure

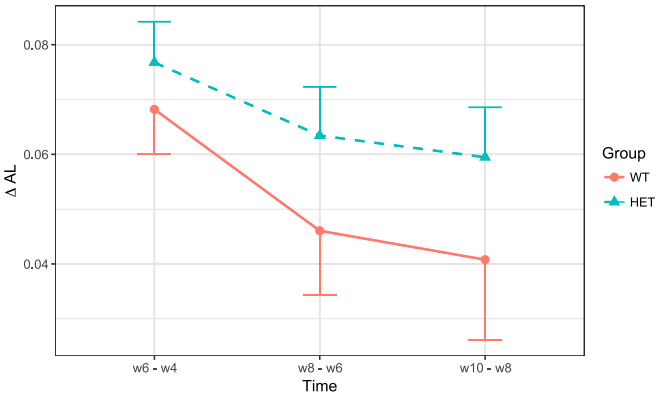

Fig. 3. Clinical features of the *Bsg* mutant mice. Comparisons of the ALs in the WT and mutant mice at each time point [week 6 (w6)–w4, w8–w6, w10–w8]. HET, heterozygous mutant mice; WT, wild-type mice.

to environmental risks, we designed this study using a special cohort with EOHM. Each trio has one EOHM child and two unaffected parents, with or without another unaffected sibling. Through this design, we were able to focus on the genetic cause of the newly created EOHM in each family.

Our study used a trio-based WES strategy to dissect the genetic basis of EOHM. Based on WES and the subsequent validation, we deciphered the genetic causes of 4 known genes and discovered 12 unique candidate genes. A total of 16 biallelic or de novo mutations were identified in the present study. To date, cohort-based genetic studies have identified several genes that contribute to myopic development. Jiang et al. (25) comprehensively screened the *LRPAP1*, *CTSH*, *LEPREL1*, *ZNF644*, *SLC39A5*, and *SCO2* genes in 298 families with EOHM and identified potential pathogenic mutations in 9 patients, with a detection rate of 3.02% (9/298). Among these genes, *ZNF644* was the major gene of EOHM (1.67%, 5/298), whereas no mutations were identified in *CTSH* and *LEPREL1*. Collectively, these results suggested that the genetic defects responsible for most cases remain to be determined. Strikingly, we deciphered a significant rate of the genetic causes in these trios, supporting our initial hypothesis that EOHM is mainly driven by genetic predisposition.

Among the rare inherited biallelic mutations, three mutations were identified in the known genes *GRM6*, *CACNA1F*, and *FAM161A* that are responsible for inherited retinal dystrophy (IRD) (Dataset S1). Interestingly, HM occurs concomitantly in IRD patients with *GRM6* or *CACNA1F* mutations (32, 62). Our findings are consistent with a previous study showing that 23.8% (71/298) of patients with EOHM actually harbor mutations in *IRD* genes (38).

The role of de novo mutations in EOHM onset has never been explored. In this study, a total of 20 de novo mutations in the

Table 1. Summary of *BSG* mutations and the associated phenotypes identified in this study

						Refractive errors (DS)		BCVA	
Patient ID	Mutation (zygosity)	ExAC	EVS	1000G	Type (damaging score*)	OD	OS	OD	OS
H13	c.889G>A, p.G297S (het)	1/115742	None	None	Missense (12/14)	−9.00	−8.50	0.6	0.6
T100	c.661C>T, p.P221S (het)	None	None	None	Missense (9/14)	−6.00	−7.00	0.8	0.8
HM850	c.415+1G>A (het)	None	None	None	Splicing	−11.50	−12.00	0.3	0.3
M487	c.205C>T, p.Q69X (het)	None	None	None	Nonsense	−11.00	−9.25	1.0	1.0
M813	c.205C>T, p.Q69X (het)	None	None	None	Nonsense	−7.25	−9.00	1.0	1.0

BCVA, best-corrected visual acuity; DS, diopters; EVS, Exome Variant Server; ExAC, Exome Aggregation Consortium; 1000G, 1000 Genomes Project; OD, right eye; OS, left eye.
*Damaging score: Damage prediction of missense mutation using 14 online tools (Polyphen2_HDIV, Polyphen2_HVAR, MutationTaster, SIFT, LRT, MutationAssessor, FATHMM, RadialSVM, LR, VEST3, CADD, GERP++, phyloP100way, and SiPhy_29way).

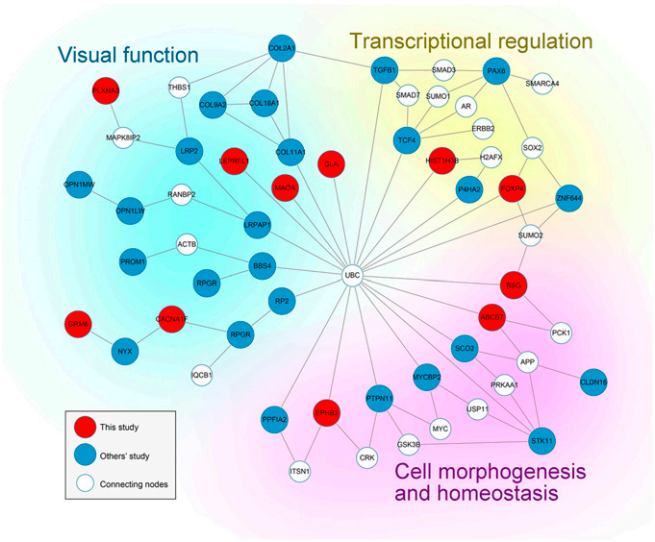

Fig. 4. PPI of the HM genes. PPI network of the genes related to HM identified in this study and previous studies.

coding regions were validated in 12 EOHM probands. Interestingly, the de novo mutation rate was significantly elevated in the probands compared with that in the normal subjects (RR = 1.51, 1.11 vs. 0.74, $P = 0.05$), in particular damaging missense mutations (RR = 3.74, 0.39 vs. 0.1, $P = 0.004$). In addition, the de novo mutation rate was positively correlated with paternal age in this study (Fig. 1*B*). Children's refractive changes decrease with parental reproductive age (63), and thus, we speculate that the increased de novo mutation rate in the subjects with aged parents may be the underlying reason for the disease. In fact, we successfully identified several EOHM candidate genes with identified de novo mutations, such as *BSG*, *EPHB2*, *CSMD1*, and *TENM4*. These findings suggest that de novo mutations contribute substantially to the genetic etiology of EOHM.

The identification of recurrent de novo mutations serves as a useful method to identify disease-causing genes. However, we found that all of the de novo mutations occurred in different genes, which prevented us from performing a statistical analysis of these genes. Then, we searched the genes carrying damaging de novo missense mutations against the literature and found that none of them was associated with HM in previous reports, which can be explained by the fact that de novo mutations are extremely rare events that cannot be identified by GWAS or a linkage analysis. We subsequently asked whether there are any functional categories or cellular pathways enriched in this study. Despite the substantial genetic heterogeneity in HM, closely interconnected protein–protein interactions (PPIs) were identified by integrating the HM risk genes obtained from this and previous studies (Table S4). A gene ontology (GO) enrichment analysis showed that 43 of 62 genes were jointly clustered in four GO biological processes (Table S5). The results suggest that these genes play important roles in disease predisposition. The PPI analysis of these genes revealed a highly connected network, implying that EOHM is associated with visual perception, transcriptional regulation, and cell morphogenesis and homeostasis (Fig. 4).

Among these genes with de novo mutations, we discovered a de novo mutation in a unique gene, *BSG*, in patient H13, and identified three different *BSG* mutations in an expanded screen of 1,040 patients with HM. We further verified its functional impact by generating knockin mice carrying the same *BSG* mutation identified in the first EOHM patient. Strikingly, the mutant mice displayed the myopic feature of an enlarged AL. In addition, our results showed that the spatial expression pattern of *Bsg* is similar to other known genes, such as *Sco2* and *Sntb1* (64, 65). *BSG* encodes basigin, which is associated with retinal development and function. A previous study showed that *Bsg* KO mice led to defective function and photoreceptor degeneration in the retina (58, 59). Interestingly, Basigin plays an important role in mediating the binding of rod-derived cone viability factor (*RdCVF*) to the glucose transporter GLUT1, which increases glucose influx into cone photoreceptors (66). This evidence indicated that the retina might be one of the disease target tissues in EOHM driven by the *BSG* mutation. In this study, the *Bsg* mutant mice displayed the typical HM phenotypes with AL. As AL is responsible for myopia development (67), our results indicate that the *Bsg* mutation predisposed typical myopic phenotypes.

In summary, we performed a trio-based study to genetically dissect EOHM using next-generation sequencing and deciphered an important role for de novo mutations in this disease. The discovery of a disease gene, *BSG*, provides insight into myopia development and etiology, which expands our current understanding of HM and might be useful for future treatment and prevention.

Methods

The human subjects were recruited from The Eye Hospital of Wenzhou Medical University in accordance with a protocol approved by the Ethics Committee of the hospital. Written informed consent was provided by the parents and on behalf of their children before the peripheral blood, and clinical data were collected from the myopia patients and their parents. The experimental procedures are described in detail in *SI Methods*.

ACKNOWLEDGMENTS. We thank the families for participation in this study. This study was supported by National Key Basic Research Program Grant 2013CB967502; National Natural Science Foundation of China Grants 81522014, 81371059, and 81500741; Zhejiang Provincial Natural Science Foundation of China Grant LR13H120001; Zhejiang Provincial Key Research and Development Program Grant 2015C03029; Wenzhou Science and Technology Innovation Team Project Grant C20150004; MOST Projects Grant 2012YQ12008004; National Institutes of Health/National Eye Institute (NIH/NEI) Grants 1R0 1EY018246-01 and R01 EY014685; Research to Prevent Blindness, Inc.; and University of Wisconsin School of Medicine and Public Health Centennial Scholars Fund.

1. Morgan IG, Ohno-Matsui K, Saw SM (2012) Myopia. *Lancet* 379:1739–1748.
2. Morgan I, Rose K (2005) How genetic is school myopia? *Prog Retin Eye Res* 24:1–38.
3. Pan CW, Ramamurthy D, Saw SM (2012) Worldwide prevalence and risk factors for myopia. *Ophthalmic Physiol Opt* 32:3–16.
4. Bourne RR, et al.; Vision Loss Expert Group (2013) Causes of vision loss worldwide, 1990–2010: A systematic analysis. *Lancet Glob Health* 1:e339–e349.
5. Young TL, Metlapally R, Shay AE (2007) Complex trait genetics of refractive error. *Arch Ophthalmol* 125:38–48.
6. Hornbeak DM, Young TL (2009) Myopia genetics: A review of current research and emerging trends. *Curr Opin Ophthalmol* 20:356–362.
7. Saw SM, Katz J, Schein OD, Chew SJ, Chan TK (1996) Epidemiology of myopia. *Epidemiol Rev* 18:175–187.
8. He M, et al. (2015) Effect of time spent outdoors at school on the development of myopia among children in China: A randomized clinical trial. *JAMA* 314: 1142–1148.
9. Rose KA, et al. (2008) Outdoor activity reduces the prevalence of myopia in children. *Ophthalmology* 115:1279–1285.
10. Lee KE, Klein BE, Klein R, Fine JP (2001) Aggregation of refractive error and 5-year changes in refractive error among families in the Beaver Dam Eye Study. *Arch Ophthalmol* 119:1679–1685.
11. Wojciechowski R, et al. (2005) Heritability of refractive error and familial aggregation of myopia in an elderly American population. *Invest Ophthalmol Vis Sci* 46:1588–1592.
12. Fotouhi A, et al. (2007) Familial aggregation of myopia in the Tehran eye study: Estimation of the sibling and parent offspring recurrence risk ratios. *Br J Ophthalmol* 91:1440–1444.
13. Lam DS, et al. (2008) The effect of parental history of myopia on children's eye size and growth: Results of a longitudinal study. *Invest Ophthalmol Vis Sci* 49:873–876.
14. Lopes MC, Andrew T, Carbonaro F, Spector TD, Hammond CJ (2009) Estimating heritability and shared environmental effects for refractive error in twin and family studies. *Invest Ophthalmol Vis Sci* 50:126–131.
15. Wojciechowski R (2011) Nature and nurture: The complex genetics of myopia and refractive error. *Clin Genet* 79:301–320.
16. Verhoeven VJ, et al.; Consortium for Refractive Error and Myopia (CREAM); Diabetes Control and Complications Trial/Epidemiology of Diabetes Interventions and Complications (DCCT/EDIC) Research Group; Wellcome Trust Case Control Consortium 2

(WTCCC2); Fuchs' Genetics Multi-Center Study Group (2013) Genome-wide meta-analyses of multiancestry cohorts identify multiple new susceptibility loci for refractive error and myopia. *Nat Genet* 45:314–318.
17. Fan Q, et al. (2012) Genetic variants on chromosome 1q41 influence ocular axial length and high myopia. *PLoS Genet* 8:e1002753.
18. Aldahmesh MA, et al. (2013) Mutations in LRPAP1 are associated with severe myopia in humans. *Am J Hum Genet* 93:313–320.
19. Mordechai S, et al. (2011) High myopia caused by a mutation in LEPREL1, encoding prolyl 3-hydroxylase 2. *Am J Hum Genet* 89:438–445.
20. Shi Y, et al. (2011) Exome sequencing identifies ZNF644 mutations in high myopia. *PLoS Genet* 7:e1002084.
21. Tran-Viet KN, et al. (2013) Mutations in SCO2 are associated with autosomal-dominant high-grade myopia. *Am J Hum Genet* 92:820–826.
22. Guo H, et al. (2014) SLC39A5 mutations interfering with the BMP/TGF-β pathway in non-syndromic high myopia. *J Med Genet* 51:518–525.
23. Guo H, et al. (2015) Mutations of P4HA2 encoding prolyl 4-hydroxylase 2 are associated with nonsyndromic high myopia. *Genet Med* 17:300–306.
24. Xiao X, Li S, Jia X, Guo X, Zhang Q (2016) X-linked heterozygous mutations in ARR3 cause female-limited early onset high myopia. *Mol Vis* 22:1257–1266.
25. Jiang D, et al. (2014) Detection of mutations in LRPAP1, CTSH, LEPREL1, ZNF644, SLC39A5, and SCO2 in 298 families with early-onset high myopia by exome sequencing. *Invest Ophthalmol Vis Sci* 56:339–345.
26. Li H, Durbin R (2009) Fast and accurate short read alignment with Burrows-Wheeler transform. *Bioinformatics* 25:1754–1760.
27. McKenna A, et al. (2010) The Genome Analysis Toolkit: A MapReduce framework for analyzing next-generation DNA sequencing data. *Genome Res* 20:1297–1303.
28. Li J, et al. (2015) mirTrios: An integrated pipeline for detection of de novo and rare inherited mutations from trios-based next-generation sequencing. *J Med Genet* 52:275–281.
29. Khan AO, Aldahmesh MA, Alsharif H, Alkuraya FS (2015) Recessive mutations in LEPREL1 underlie a recognizable lens subluxation phenotype. *Ophthalmic Genet* 36: 58–63.
30. Guo H, et al. (2014) Homozygous loss-of-function mutation of the LEPREL1 gene causes severe non-syndromic high myopia with early-onset cataract. *Clin Genet* 86:575–579.
31. Hudson DM, et al. (2015) Post-translationally abnormal collagens of prolyl 3-hydroxylase-2 null mice offer a pathobiological mechanism for the high myopia linked to human LEPREL1 mutations. *J Biol Chem* 290:8613–8622.
32. Xu X, et al. (2009) Sequence variations of GRM6 in patients with high myopia. *Mol Vis* 15:2094–2100.
33. Sergouniotis PI, et al. (2012) A phenotypic study of congenital stationary night blindness (CSNB) associated with mutations in the GRM6 gene. *Acta Ophthalmol* 90:e192–e197.
34. Langmann T, et al. (2010) Nonsense mutations in FAM161A cause RP28-associated recessive retinitis pigmentosa. *Am J Hum Genet* 87:376–381.
35. Bandah-Rozenfeld D, et al. (2010) Homozygosity mapping reveals null mutations in FAM161A as a cause of autosomal-recessive retinitis pigmentosa. *Am J Hum Genet* 87: 382–391.
36. Zach F, et al. (2012) The retinitis pigmentosa 28 protein FAM161A is a novel ciliary protein involved in intermolecular protein interaction and microtubule association. *Hum Mol Genet* 21:4573–4586.
37. Zhou Y, et al. (2015) Whole-exome sequencing reveals a novel frameshift mutation in the FAM161A gene causing autosomal recessive retinitis pigmentosa in the Indian population. *J Hum Genet* 60:625–630.
38. Sun W, et al. (2015) Exome sequencing on 298 probands with early-onset high myopia: Approximately one-fourth show potential pathogenic mutations in RetNet genes. *Invest Ophthalmol Vis Sci* 56:8365–8372.
39. Upton AL, et al. (1999) Excess of serotonin (5-HT) alters the segregation of ispilateral and contralateral retinal projections in monoamine oxidase A knock-out mice: Possible role of 5-HT uptake in retinal ganglion cells during development. *J Neurosci* 19: 7007–7024.
40. Salichon N, et al. (2001) Excessive activation of serotonin (5-HT) 1B receptors disrupts the formation of sensory maps in monoamine oxidase A and 5-HT transporter knockout mice. *J Neurosci* 21:884–896.
41. Desnick RJ, Banikazemi M (2006) Fabry disease: Clinical spectrum and evidence-based enzyme replacement therapy. *Nephrol Ther* 2:S172–S185.
42. Bruner WE, Dejak TR, Grossniklaus HE, Stark WJ, Young E (1985) Corneal alpha-galactosidase deficiency in macular corneal dystrophy. *Ophthalmic Paediatr Genet* 5:179–183.
43. Michalakis S, et al. (2014) Mosaic synaptopathy and functional defects in Cav1.4 heterozygous mice and human carriers of CSNB2. *Hum Mol Genet* 23:1538–1550.
44. Hauke J, et al. (2013) A novel large in-frame deletion within the CACNA1F gene associates with a cone-rod dystrophy 3-like phenotype. *PLoS One* 8:e76414.
45. Vincent A, Wright T, Day MA, Westall CA, Héon E (2011) A novel p.Gly603Arg mutation in CACNA1F causes Åland island eye disease and incomplete congenital stationary night blindness phenotypes in a family. *Mol Vis* 17:3262–3270.
46. O'Roak BJ, et al. (2011) Exome sequencing in sporadic autism spectrum disorders identifies severe de novo mutations. *Nat Genet* 43:585–589.
47. Samocha KE, et al. (2014) A framework for the interpretation of de novo mutation in human disease. *Nat Genet* 46:944–950.
48. Girard SL, et al. (2011) Increased exonic de novo mutation rate in individuals with schizophrenia. *Nat Genet* 43:860–863.
49. Li J, et al. (2016) Genes with de novo mutations are shared by four neuropsychiatric disorders discovered from NPdenovo database. *Mol Psychiatry* 21:298.
50. Michaelson JJ, et al. (2012) Whole-genome sequencing in autism identifies hot spots for de novo germline mutation. *Cell* 151:1431–1442.
51. Francioli LC, et al.; Genome of the Netherlands Consortium (2015) Genome-wide patterns and properties of de novo mutations in humans. *Nat Genet* 47:822–826.
52. Kleinberger J, Maloney KA, Pollin TI, Jeng LJ (2016) An openly available online tool for implementing the ACMG/AMP standards and guidelines for the interpretation of sequence variants. *Genet Med* 18:1165.
53. Richards S, et al.; ACMG Laboratory Quality Assurance Committee (2015) Standards and guidelines for the interpretation of sequence variants: A joint consensus recommendation of the American College of Medical Genetics and Genomics and the Association for Molecular Pathology. *Genet Med* 17:405–424.
54. Hon GC, et al. (2014) 5mC oxidation by Tet2 modulates enhancer activity and timing of transcriptome reprogramming during differentiation. *Mol Cell* 56:286–297.
55. Ament SA, et al.; Bipolar Genome Study (2015) Rare variants in neuronal excitability genes influence risk for bipolar disorder. *Proc Natl Acad Sci USA* 112:3576–3581.
56. Anonymous; Psychiatric GWAS Consortium Bipolar Disorder Working Group (2011) Large-scale genome-wide association analysis of bipolar disorder identifies a new susceptibility locus near ODZ4. *Nat Genet* 43:977–983.
57. Nakamura H, Cook RN, Justice MJ (2013) Mouse Tenm4 is required for mesoderm induction. *BMC Dev Biol* 13:9.
58. Philp NJ, Ochrietor JD, Rudoy C, Muramatsu T, Linser PJ (2003) Loss of MCT1, MCT3, and MCT4 expression in the retinal pigment epithelium and neural retina of the 5A11/basigin-null mouse. *Invest Ophthalmol Vis Sci* 44:1305–1311.
59. Chen S, et al. (2004) Effects of flanking genes on the phenotypes of mice deficient in basigin/CD147. *Biochem Biophys Res Commun* 324:147–153.
60. Zhou X, et al. (2008) The development of the refractive status and ocular growth in C57BL/6 mice. *Invest Ophthalmol Vis Sci* 49:5208–5214.
61. Chou TH, et al. (2011) Postnatal elongation of eye size in DBA/2J mice compared with C57BL/6J mice: In vivo analysis with whole-eye OCT. *Invest Ophthalmol Vis Sci* 52: 3604–3612.
62. Hemara-Wahanui A, et al. (2005) A CACNA1F mutation identified in an X-linked retinal disorder shifts the voltage dependence of Cav1.4 channel activation. *Proc Natl Acad Sci USA* 102:7553–7558.
63. Lin Z, et al. (2015) The association between maternal reproductive age and progression of refractive error in urban students in Beijing. *PLoS One* 10:e0139383.
64. Khor CC, et al.; Nagahama Study Group (2013) Genome-wide association study identifies ZFHX1B as a susceptibility locus for severe myopia. *Hum Mol Genet* 22: 5288–5294.
65. Shi Y, et al. (2013) A genome-wide meta-analysis identifies two novel loci associated with high myopia in the Han Chinese population. *Hum Mol Genet* 22:2325–2333.
66. Aït-Ali N, et al. (2015) Rod-derived cone viability factor promotes cone survival by stimulating aerobic glycolysis. *Cell* 161:817–832.
67. Benjamin B, Davey JB, Sheridan M, Sorsby A, Tanner JM (1957) Emmetropia and its aberrations; a study in the correlation of the optical components of the eye. *Spec Rep Ser Med Res Counc (G B)* 11:1–69.